СООБЩЕНИЯ
ОБЪЕДИНЕННОГО
ИНСТИТУТА
ЯДЕРНЫХ
ИССЛЕДОВАНИЙ

Дубна

E14 - 5731

S. Deme, J. Horvath, N. Kroo,
F. Szlavik, G. Zsigmond

ЛАБОРАТОРИЯ НЕЙТРОННОЙ ФИЗИКИ

SYNCHRONIZED CHOPPER TIME-OF-FLIGHT SPECTROMETER AT THE DUBNA PULSED REACTOR IBR-30

1971

E14 - 5731

S. Deme, J. Horvath, N. Kroo,
F. Szlavik*, G. Zsigmond*

SYNCHRONIZED CHOPPER TIME-OF-FLIGHT SPECTROMETER AT THE DUBNA PULSED REACTOR IBR-30

* Central Research Institute for Physics, Budapest

I. Introduction

A time-of-flight spectrometer V-1 has been constructed at the pulsed fast reactor[1] in Dubna for inelastic scattering studies in solids. The spectrometer is based on the so called direct geometry. Neutrons are monochromatized by a chopper, synchronized and phased to the reactor. Scattered neutrons can be analysed in 8 angles simultaneously. The angular resolution of a single detector is $\pm 0.5^{\circ}$ and the angular region available for measurements $\pm 65^{\circ}$. The energy of the monochromatic neutron beam can be varied practically in all the thermal energy regions.

II. Description of the Spectrometer

The spectrometer consists of the following main parts:

a) neutron source;

b) moderator;

c) flight path of the neutrons with collimators and shielding;

d) synchronized chopper;

e) neutron detectors;

f) data collecting and processing system;

g) monitor.

The lay-out of the spectrometer is shown in Fig. 1.

a) Neutron source. The neutron source for the V-1 spectrometer is the IBR-30 reactor. Its main parameters are summarized in Table I. If it is operated in the so called reactor regime, the neutron burst repetition frequency can be chosen as 4; 5 and 10 c/s. In a special regime of rare pulses 1/3.8 and 1/7.6 c/s frequencies can be used. The reactor can be operated as a booster triggered by a linear electron accelerator. The repetition frequency in this case is 100 c/s. The full widths at half height of the neutron burst in the reactor regime is 55 μs and its shape is shown in Fig. 2. The burst width in the booster regime depends on the multiplication factor of the system and is about 3-4 μs .

The repetition frequencies, given above, are realized when the speed of the main rotor is 3000 c/s. In fact, this speed can be varied in the 2200-3000 c/s region. The burst repetition frequencies vary linearly with the speed of the main disc.

b) Moderator. Generally 4 cm thick layer of water is used to slow down the fast neutrons. The effective surface of the moderator is 45 x 28 cm^2 and its geometry is shown in Fig. 3. The equilibrium temperature of the water layer is about 50°C. The normalized distribution of neutrons in wavelength scale is shown in Fig. 4. as measured on a 16.7 m long flight path in the 0.5 - 4 Å region. The time distribution of 3.8 Å neutrons is shown in Fig. 5. If neutrons of the cold region are needed a combined liquid N_2 cooled polyethylene - Be moderator can be used.

c) Flight path. The distance of the sample from the point A (see on Fig. 3) of the moderator can be given as 982 cm. Part of this path is in the reactor hall, another one in the water-shutter which is evacuated during the measurements and finally the third part is in the experimental hall surrounded by water and paraffin filled shieldings. Before the chopper a concrete shutter is located with a collimator in it which can be moved into the beam during measurements. The opening of the collimator is 7.5 x 7.5 cm and its divergency is chosen so that the chopper window is seen from each point of the moderator. The flight path of scattered neutrons is shielded by a truncated pyramid shaped tube filled with Ar gas at a bit higher than 1 at pressure. The total distance between the moderator and the detectors is 1680 cm, 50% it contains air, 14% is evacuated and 36% argon filled.

The D.C. motor which rotates the chopper has a specific small diameter rotor. It has outer excitation with a commutating pole. The speed is proportional with the voltage on the rotor. The power at 7500 rev/min is as high as 1.2 kw. The maximum rotor voltage is 110 V.

The chopper is housed in a Cd cased steel tube with 0.1mm Al windows for the incoming and outgoing neutron beams.

The start signals for the two slit systems are given by magnetic pick-ups which are fixed to the chopper house. Each pick-up consists of a ductile iron shoe, soldered to a $\phi 4$ mm magnetic ALNICO rod and covered by a coil (Cu , ϕ 0.08 mm, about 500 turns). The U shaped magnet and ductile iron shoe is closed by the steel disc on the chopper rotors and broken by a narrow slit on it when the chopper is open for the neutrons. The rise time of the pick-up pulse at 6000 rev/min chopper speed is about 3–4μs, which triggers a blocking circuit.

The chopper is located far from the source, as seen in Fig.1, and can therefore be used as a neutron monochromator. That means it has to be phased to the reactor. In order to get good resolution the requirements for this phasing are severe. The block diagram of the stabilizing system is shown in Fig. 8. Its working principle can be understood from Fig. 9. The oscillator which is synchronized to the reactor start pulsed gives afterwards digitally delayed (0 - 100 ms) internal start pulses (a). These pulses are used to start saw-tooth pulses (b) with T_f period time. If the time of the chopper start pulse does not coincide with the $T_f/2$ moment the comparator circuit produces an error signal proportional to the Δt time difference. This signal corrects the current of the motor. The phase stability of the system is $\pm$ 10 μs .

e) <u>Neutron detectors.</u> The scatterd by the sample neutrons are detected in SNM-33 type ^{3}He counters/2/. The effectivity calculated from the known pressure and cross section data is given in Fig. 10. Eight detector banks are housed at the end of the flight path about 1.3° from each other. Each bank consists of the 3 counters. The house of the banks is made of 1 mm thick Al with 0.5 mm Cd on the outer surface. The free window in this Cd cover for neutrons to fall on the detectors is 34 cm high and 10.5 cm wide. The preamplifiers are also mounted within the detector bank boxes.

f) Electronics chains of the detectors[3]. The detector signals are amplified by the NV-224 type (KFKI Hungary) preamplifiers which are matched to the wave impedance of the used cables. The main parameters of the pre-amplifiers are as follows.

Nominal amplification 100, 200, 400.

Input and output signal polarity: negative.

Input impedance: max250 kohm || 35 pF .

Dynamic range (for 75 ohm ballast impedance) : 3V.

Rise time 0.4 μs.

Noise related to the input < 400 μV p–p .

The pre-amplifier is coupled to NK-213 type (KFKI Hungary) amplifiers + discriminators. The amplification can be varied from 0.2 till 20 in 13 steps and with continuous variation within the steps. The discriminator level is fixed at 0.75 V. The output signal is negativ and can be varied in the 3 - 15 V range. The width of this signal is $(6 \pm 0.5)\,\mu s$ with a $< 0.4\,\mu s$ rise time. The dead time of the discriminator is not higher than 10 μs . The discriminator pulses are fed into a coding unit which transfers the signals of the 8 detectors on four 600 m long 75Ω coaxial cables into a data collecting centre. After decoding the pulses are fed into a TENSOR type (USSR) 4096 channel time analyzer. The channel length can be chosen as $2^n\,\mu s$ where $n = -2 \div 6$. The dead time of the analyzer is 30 μs . The correction for this is given in Fig. 11.

The analyzer is in off-line connection with a BESM-4 type (USSR) computer which can be used to store and handle the collected data. This computer is equipped with a light pen which makes the data handling more convenient.

g) Monitor counter. An SNM-3 type, low efficiency BF_3 counter serves in the spectrometer as a monitor. It is located at the top of the chopper house in Cd discs with a hole inside and filled with the mixture of boron carbide and paraffin. The diameter of these diameter of the hole is 5.5 cm (Fig. 12). The counting rate of the monitor can be regulated by its height.

The electronic units for the monitor counter are identical with those of the detectors. A binary preset scaler is used to collect monitor counts. The counting rate at 25 kw mean reactor power is in the order of 1000 count/min. The preset scaler can block the detector pulses and so the data collection in the analyser . If the chopper falls out of phase due to some false pulse both the monitor and the analyzer are blocked. The dead time of the monitor is less than $10\,\mu s$.

III. Calculated and Measured Parameters of the Spectrometer

The following parameters of the spectrometer are calculated:

a) Neutron flux at the sample.

b) Sample-detector solid angle.

c) Time resolution.

d) Energy resolution.

a) Neutron flux at the sample. The neutron flux Φ_0 (in 2π solid angle) at the surface of the H_2O moderator is 5×10^{10} n/cm^{2}sec (at 25 kw mean power of the reactor)/1/. The surface seen by the sample is $F = 28 \times 45 = 1260$ cm^2. As the distance R_s of the sample from the moderator is 982 cm the flux can be given as

$$\phi_s = \frac{\phi_0 \cdot F}{2\pi R_s^2} \approx 10^7 \text{ n/cm}^2 \text{ sec} .$$

Let us calculate now the attenuation of the neutron beam in the chopper. The flux after the chopper can be given as

$$\phi'_s = \phi_s \cdot K(T_d) \cdot E_{eff} \; \Delta T_{1/2} \; K_t \; ,$$

where $K(T_d)$ is the spectral density of neutrons as a function of the T_d phase difference between the reactor and the chopper burst. T_d is proportional with the wavelength of the neutrons (Fig. 4).

F_{eff} is the effective surface fraction of the chopper slits, i.e. for the I system F_{eff} = 0.89 and for the II system F_{eff} = 0.87. $\Delta T_{1/2}$ is the full width at half height of the chopper time burst (Fig. 13) and K_t stands for the relative transmission function of the slits (see Fig. 14).

Let us now calculate the intensity of 1.25 Å neutrons.

As $Td_d\,[ms] = 2.38\ \lambda\,[\text{Å}]$

$$T_d = 2.38 \times 1.25 = 3\ ms\ .$$

According to Table II the proper slit-system to be used is the N^0 II one. The optimal speed of the rotor can be calculated from

$$n_{opt}\ [rev/min] = \frac{15\ v_0[cm/s]}{R[cm]}\ ,$$

where $v_0\ [cm/s] = \dfrac{3.95 \times 10^5}{\lambda[\text{Å}]}$ the velocity of the neutron with wavelength λ .

In the given case n_{opt} = 5000 rev/min. As the chopper has to be rotated at a speed which is a multiple of the reactor burst frequency (240/min) n = 4800 rev/min is the best choice. Therefore

$$\frac{\lambda}{\lambda_0} = \frac{5000}{4800} = 1.04\ ,$$

where according to Fig. 14 K_t 1 can still be taken. As ϕ_s = = 10^7 n/cm^{2}sec, $K(T_d)$ = 0.33 from Fig. 4 and $\Delta T_{1/2}$ = 23.5×10^{-3} ms from Fig. 13.

$$\phi_s' = 6.75 \times 10^4\ n/s$$

and for a 49 cm^2 sample the incoming monochromatic intensity

$$J_{sample} = 3.3 \times 10^6\ n/s\ .$$

Let us now compare this intensity with that measured. For this the scatterd by a plexiglass sample neutrons were used. In order to calculate the intensity from the measured data the solid angle of the detectors is needed.

b) Sample-detector solid angle. The distance of the detectors from the sample is 683 cm and the effective surface of the banks consisting of ^3He counters can be calculated as 34 x 3.1 x 3 = = 316 cm^2. Therefore the solid angle K_g = 316/4π x 683^2 = = 5.4 x 10^{-5}. The intensity of elastically scattered by a 2 mm thick plexiglass sample is 5.4 n/s at θ = 12.6° scattering angle. When taking the efficiency of the counters for 53 meV neutron energy (T_d = 3 ms) from Fig. 10 as η = 0.88 we get the intensity of the monochromatic neutron beam at the sample site as 5 x 10^6 n/s.

c) Time resolution of the spectrometer. The time resolution of the spectrometer can be given as

$$\Delta T_{sp}^2 = (\Delta T^*_{ch}) + (\Delta T_{det})^2 + (\Delta T_a)^2 ,$$

where ΔT^*_{ch} is the chopper burst time taking into account the geometry of the moderator as given in Fig. 13.

ΔT_{det} is the average flight time of the studied neutrons in the detectors and ΔT_a the channel width of the analyzer.

The definition of ΔT^*_{ch} is given in Fig. 15, if we suppose that the shape of the chopper burst is a triangle and the final size of the moderator surface is reflected in a rectangle. As the width of the chopper burst is smaller than that of the reactor burst width, the difference in ΔT^*_{ch} for the two slit systems can be neglected.

ΔT_{det} depends on the velocity (wavelength) of the neutrons and this dependence is shown in Fig. 16.

d) The energy resolution of the spectrometer. The energy resolution of the spectrometer is defined as

$$\frac{\Delta E}{E} \approx 2 \frac{\Delta \lambda}{\lambda} \approx 2 \frac{\Delta T^*_{ch}}{T_d} ,$$

where T_d is the flight time of the neutrons with wavelength λ from the moderator to the chopper. In the finite length of the reactor burst ΔT_R is also taken into account the resolution can be approximated by the

$$\frac{\Delta\lambda}{\lambda} = \frac{1}{T_d}\sqrt{(\Delta T^*_{ch})^2 + (\Delta T_R)^2}$$

expression although this function gives a worse resolution than the real one. If 1.31 Å neutrons are used which are passing the II chopper slit system at 6000 rpm speed of the rotor

$$\frac{\Delta\lambda}{\lambda} = 4.0\ \% .$$

In the cold neutron region the resolution becomes very high and therefore small energy transfers can be effectively studied.

The measured resolution at λ = 1.31 Å s shown in Fig. 17. The agreement with the calculated resolution is satisfactory.

IV. Conclusions

We managed to build a spectrometer for inelsatic neutron scattering studies with flexible parameters. The energy of incoming neutrons can be varied in the 3 - 130 meV and the κ -value of scattered neutrons in the 0.1 - 10 $Å^{-1}$ range. The good angular and in the case of slow neutrons high energy resolution seems to be useful for the study of the dynamics of pure and doped magnetic systems. In fact, the spectrometer was constructed with the aim of doing this type of experiments. Both incoherent and coherent scattering studies are planned first of all in the field of impurity mode studies and in magnetic phase transitions.

The authors are indebted to Mr. F. Forgacs and Mr. S. Horvath for the valuable technical assistance.

References

1. V.D. Ananjev et al. JINR Preprint, 13-4395, Dubna (1969), in Russian.
2. V.I. Korolev et al. Pribori i technika eksperimenta, No. 4, p. 46, 1970.
3. F. Szlavik et a., KFKI Report 4095/1968.

Received by Publishing Department
on April 7, 1971.

Table I

Main parameters of the IBR-30 reactor

A) Reactor regime.

Mean power (planned)	30 kw
Peak power (at 5 pulses/sec)	120 Mw
Length of the reactor pulse	60 μs
Volume of active zone	3 l
Length of the thermal pulse	90 μs
Flux of fast neutrons in the zone	
a) mean	10^{13} n/cm^{2}sec
b) peak	5×10^{16} n/cm^{2}sec

B) Booster regime.

Mean power (max.)	6 kw
Peak power (at 100 imp/sec)	30 Mw
Length of the pulse	2-3 μs
Multiplication	100-200

Table II

Design parameters of chopper

Data	Dimensions	Slit system N°I (upper)	Slit system N°II (lower)
Rotor diameter, D	cm	20	20
Slits curvature, r_0	cm	150	300
Slit width, b	cm	0.275	0.235
Wall width, h	cm	0.035	0.035
Slit-window height, H	cm	7.0	7.0
Slit-window width, M	cm	7.2	7.2
Transmission, b/(b+h)		0.89	0.87
Open time half-width, $1/2\ T/T_0$		2.2×10^{-3}	1.87×10^{-3}
Transmission half-width, (v_0/v)min/max		1 ± 0.38	1 ± 0.65
Rotational speed, n	rpm	2400-6000	2400-6000
Neutron velocity range, v_0	m/s	760... 1900	1520... 3800
Neutron wavelength range,	Å	5.2... 2.1	2.5... 0.6
Neutron energy range, E_0	meV	3... 19	11.5... 130
Slits curvature max., ϱ_1	cm	153.6	303.6
Slits curvature middle, ϱ_0	cm	150.0	300.0
Slits curvature min., ϱ_2	cm	146.4	296.4
Mass center deviation, a	cm	0.13	0.04

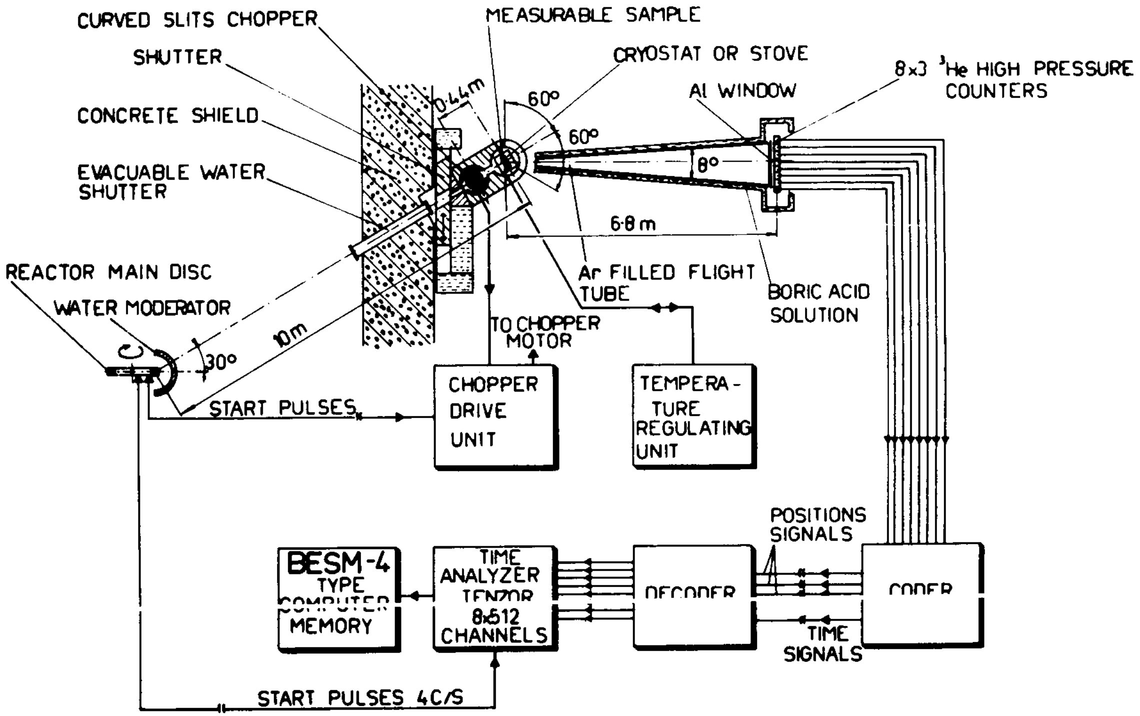

Fig. 1. Lay-out of the V-1 phased chopper time-of-flight spectrometer.

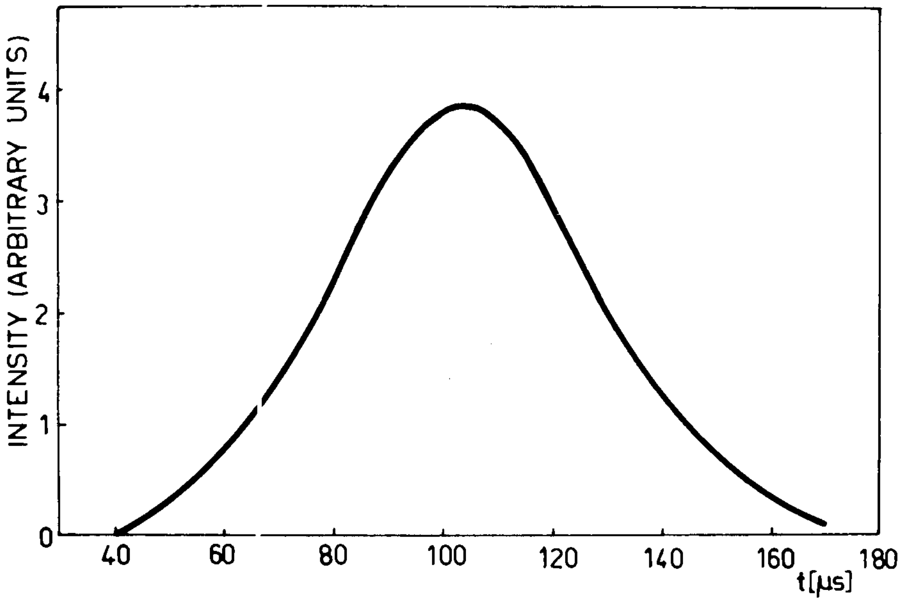

Fig. 2. The shape of the reactor burst.

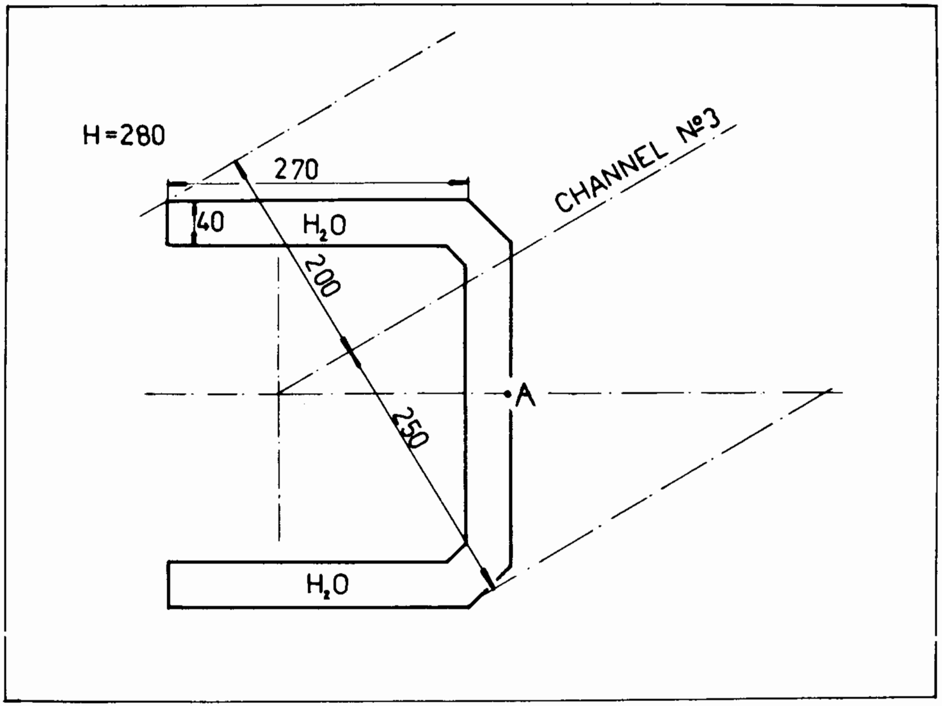

Fig. 3. The geometry of the water moderator around the fast pulsed reactor's active zone.

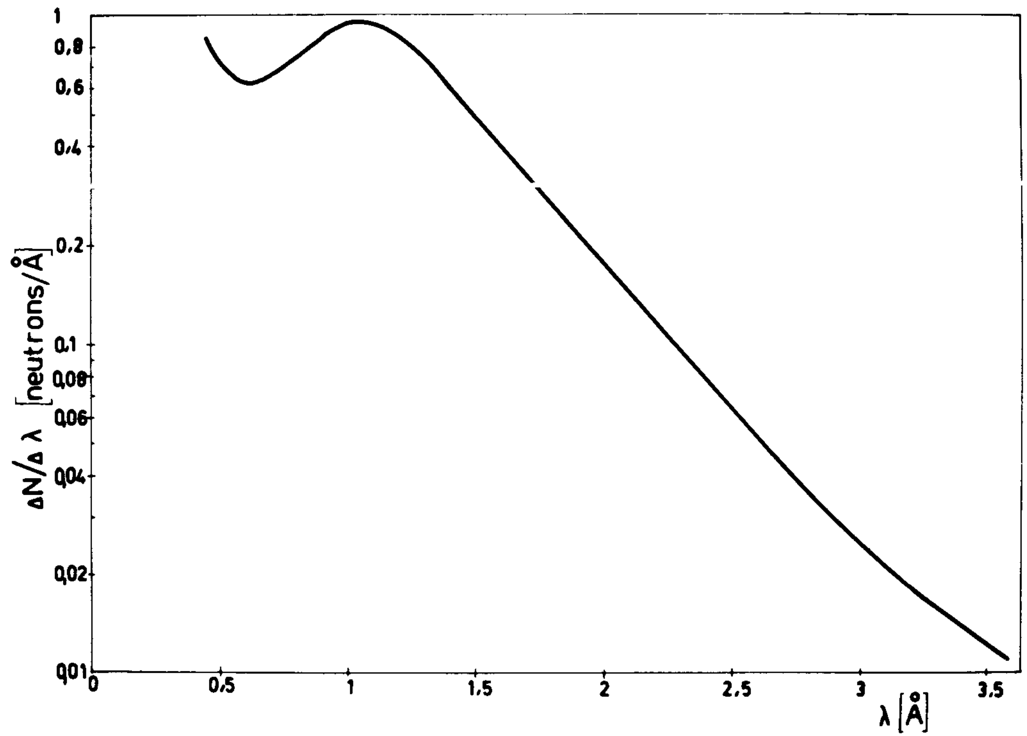

Fig. 4. Spectral density distribution of the thermal neutrons as measured by a thin detector 16.7 m from the active zone.

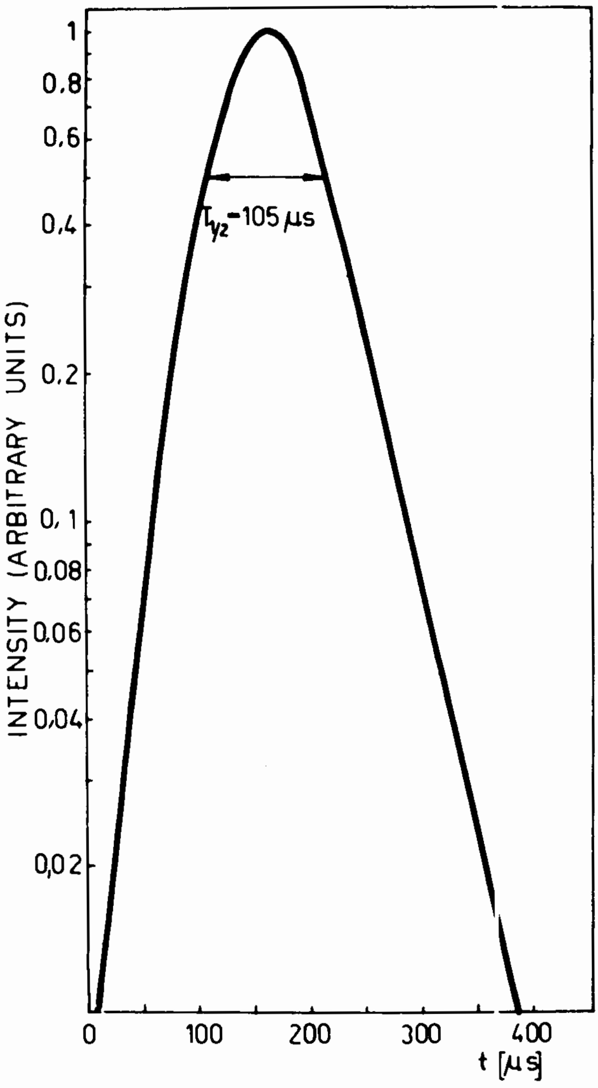

Fig. 5. Time distribution of monochromatized by the chopper 3.8 Å neutrons measured at the detector site with a small detector.

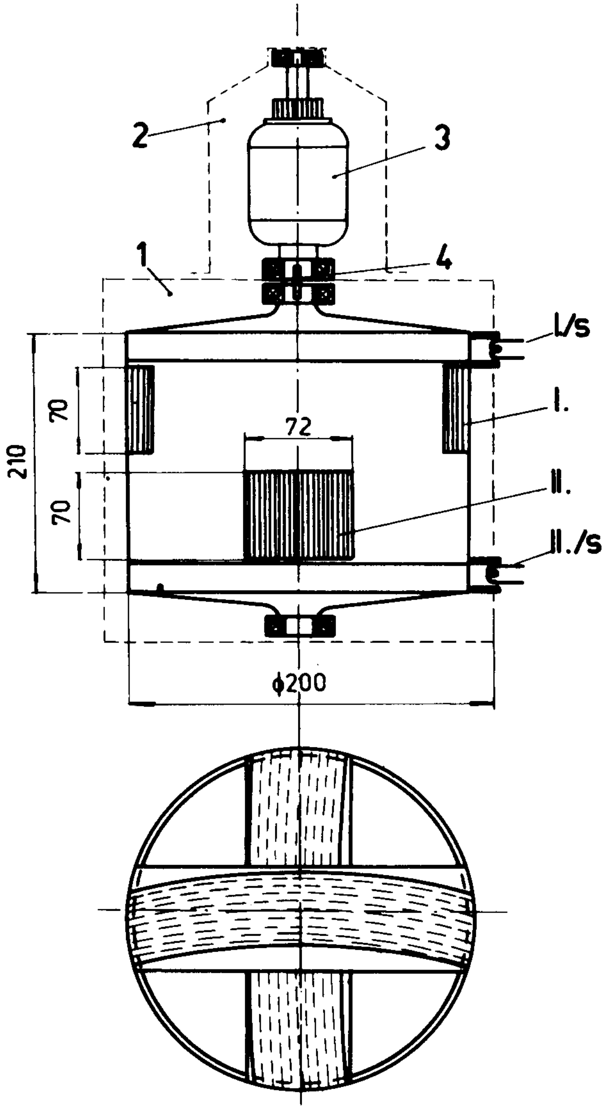

Fig. 6. Sketch of the two-slit rotor chopper. I, II slits; I/s, II/s magnetic pick-up; 1 chopper house; 2 motor house; 3 motor; 4 elastic coupling.

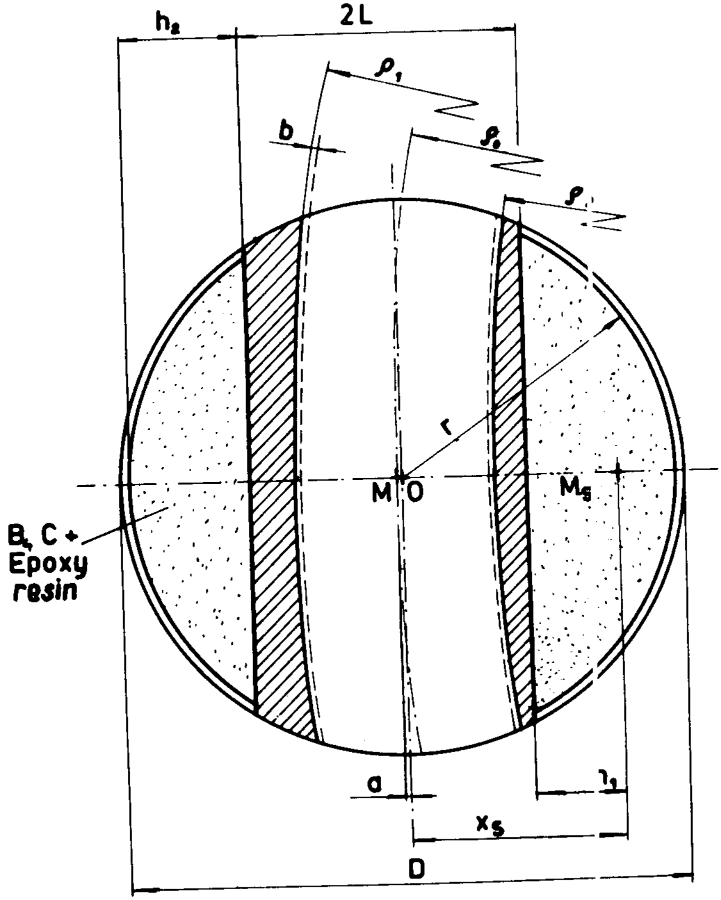

Fig. 7. Perpendicular to the rotation axis section of the rotor.

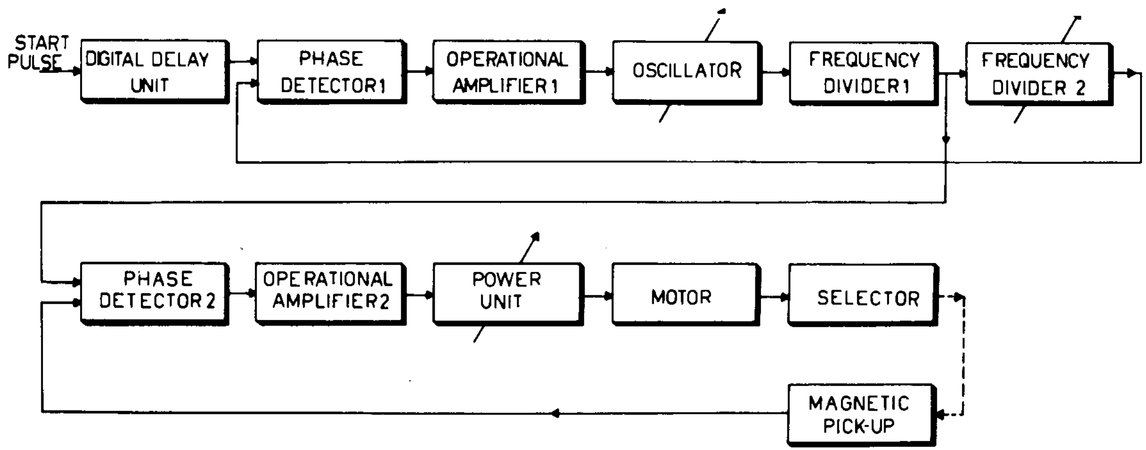

Fig. 8. Block diagram of the chopper phasing unit.

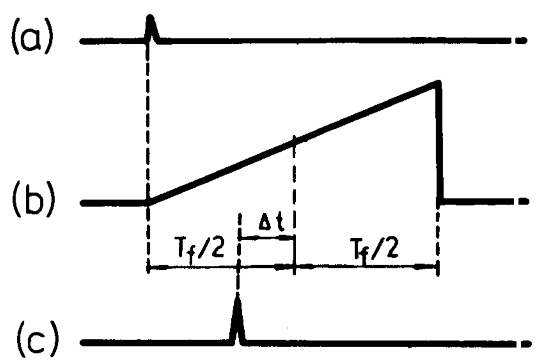

Fig. 9. Working principle of the chopper stabilizer.

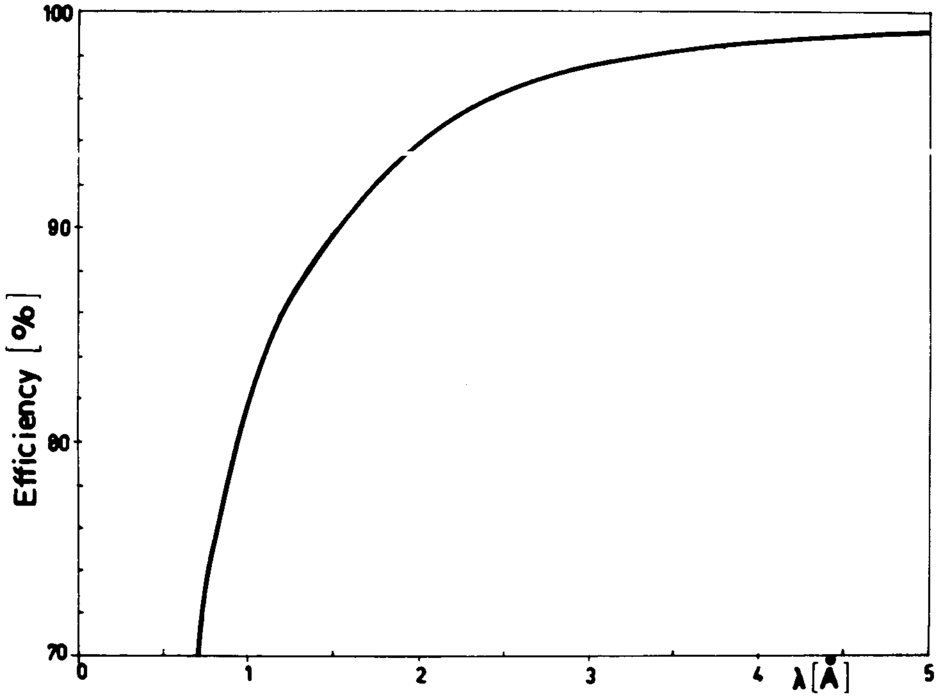

Fig. 10. Wavelength dependence of the ^{3}He counters efficiency.

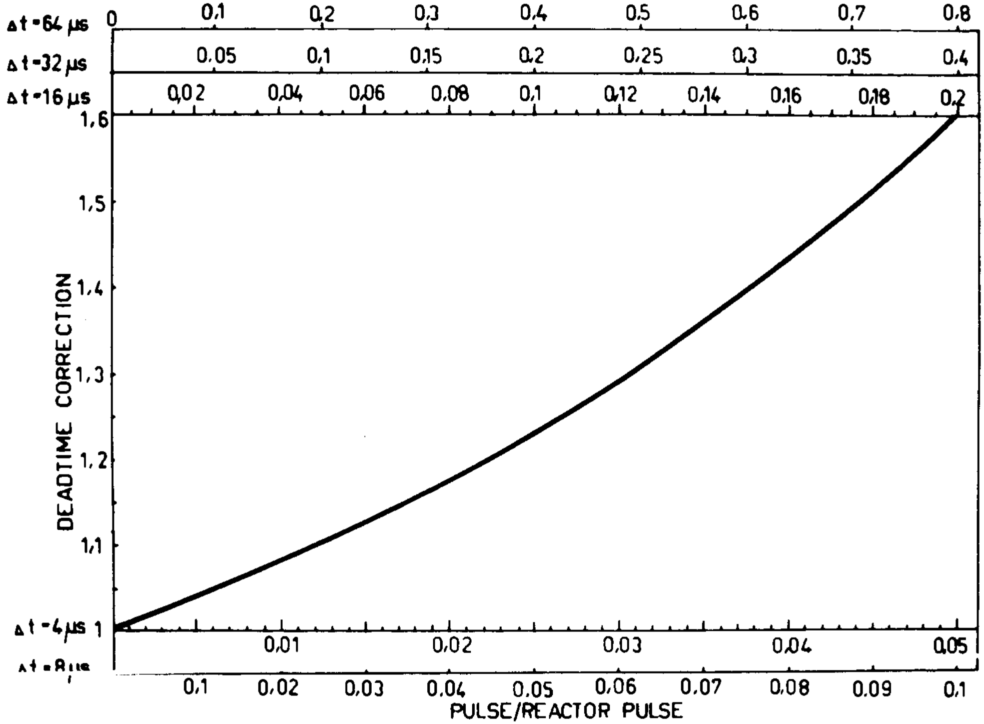

Fig. 11. Dead time corrections for the detectors.

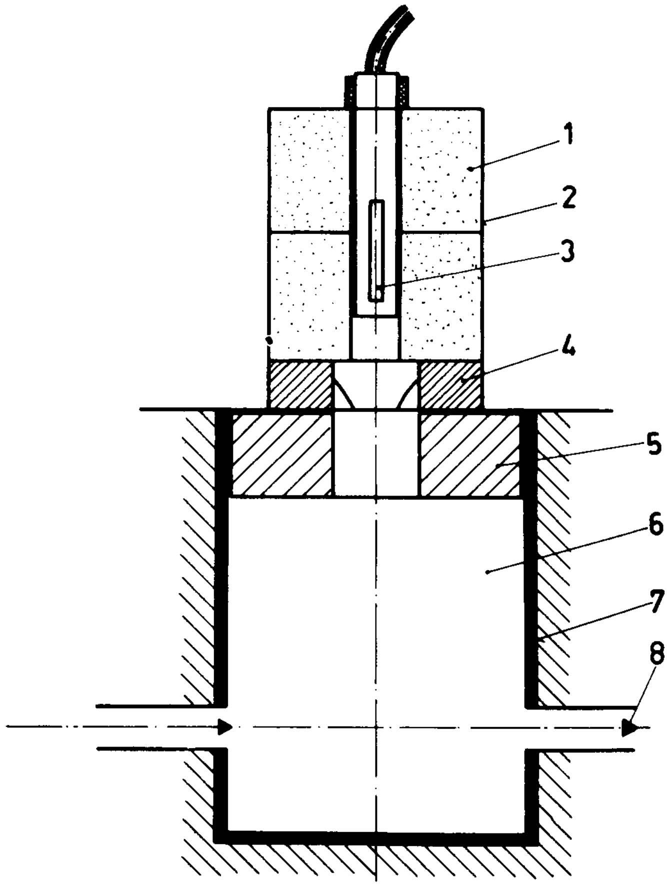

Fig. 12. Geometry of the monitor counter and its shielding. 1. Paraffin + 5% B_4C; 2. Cd box; 3. SNM-3 proportional boron counter; 4. Plastic ring; 5. Top of chopper shielding; 6. Chopper house; 7. Lead shield; 8. Neutron beam.

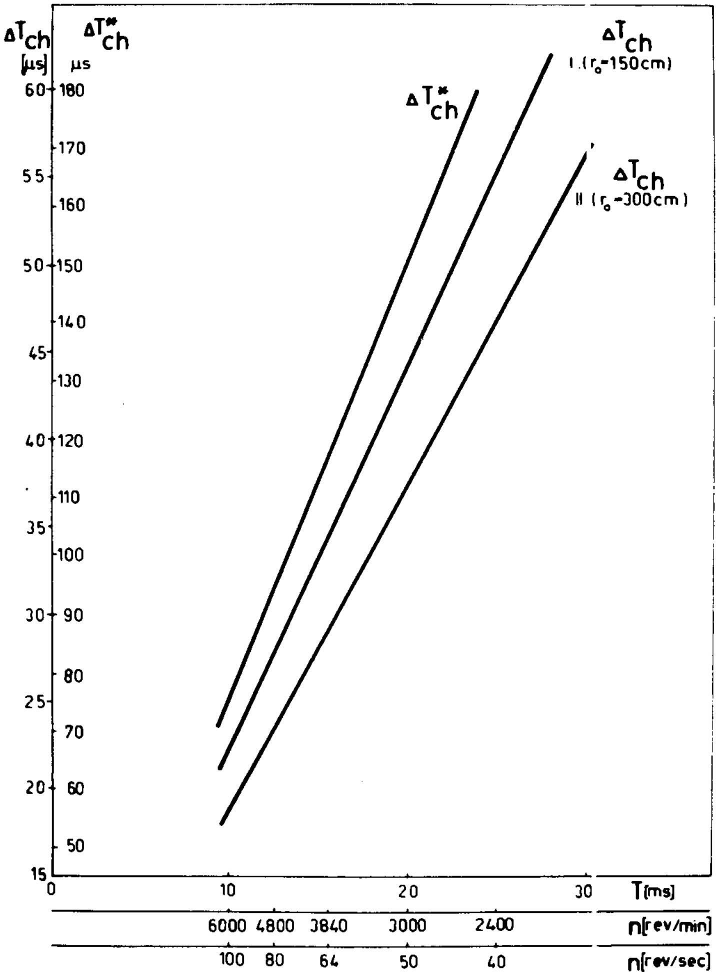

Fig. 13. The full width at half height of the chopper burst time Δt_{ch} as a function of the rotor speed. The ΔT^*_{ch} modified burst time is also shown.

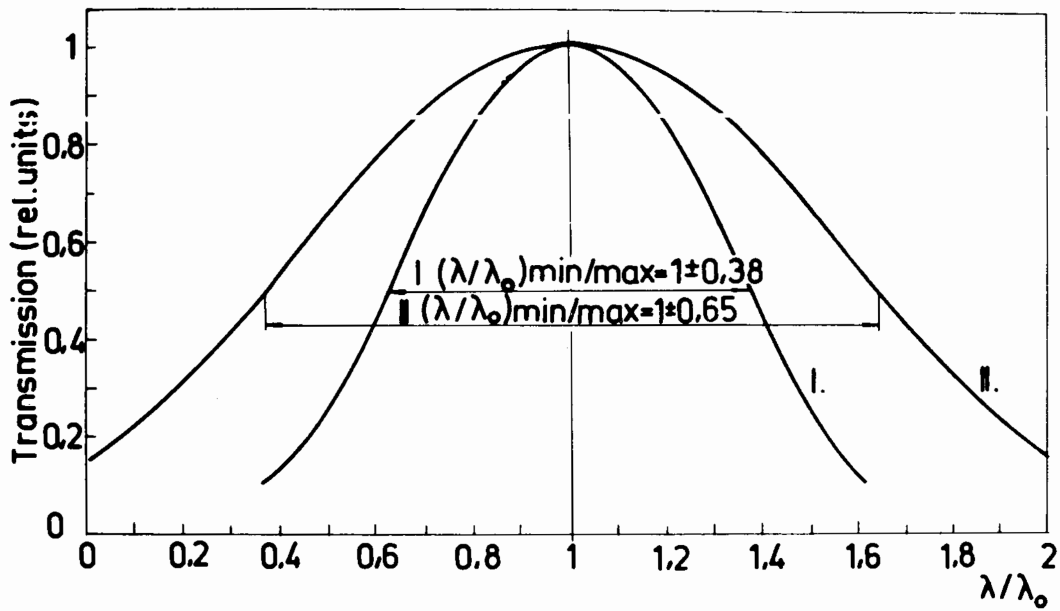

Fig. 14. Transmission function of the chopper vs λ/λ_0 .

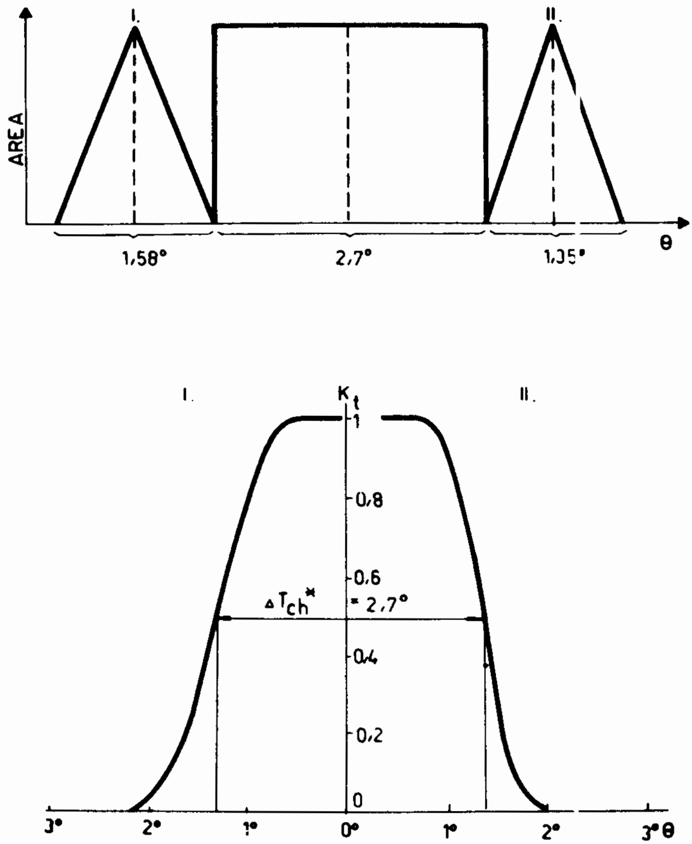

Fig. 15. The definition of ΔT^*_{ch}. The plot is given as a function of the chopper angle.

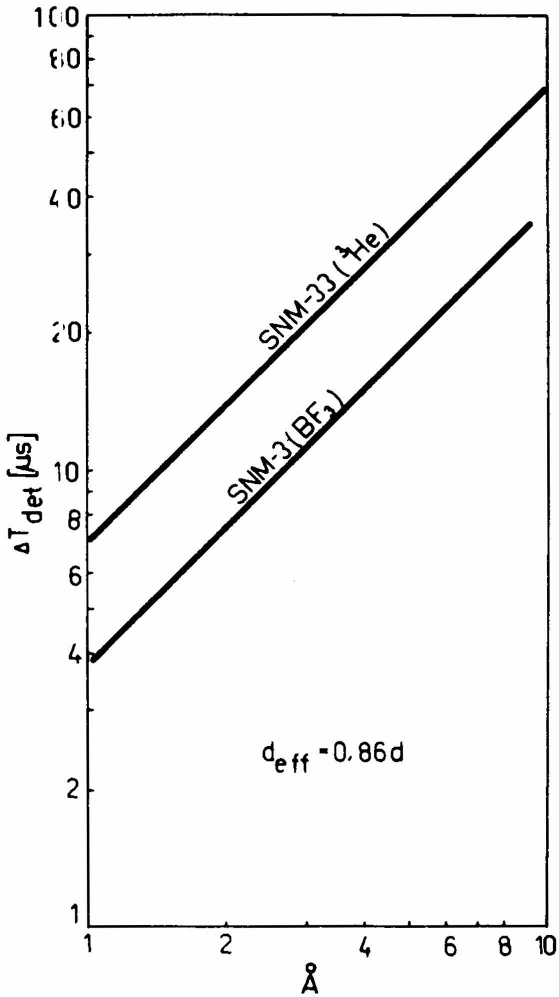

Fig. 16. ΔT_{det} as a function of the neutron velocity.

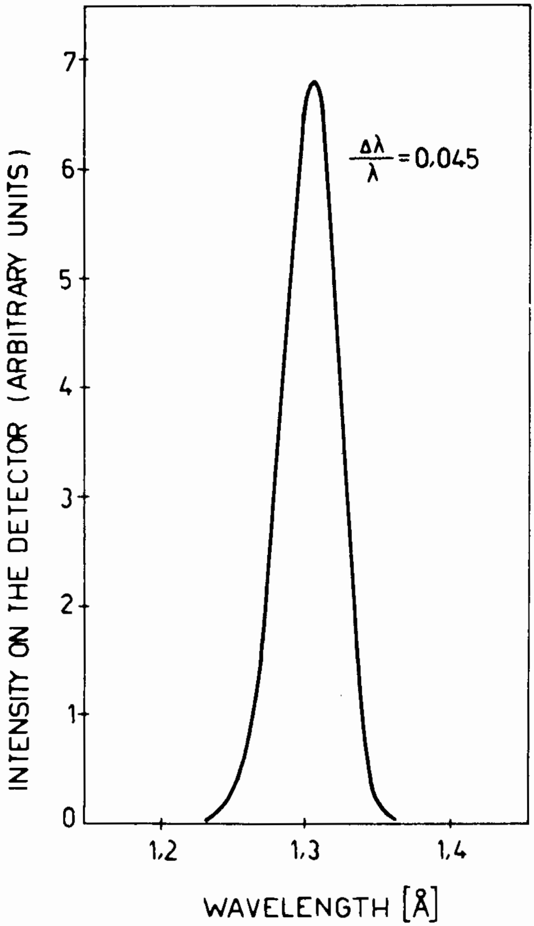

Fig. 17. Measured energy resolution function at $\lambda = 1.31$ Å.